

Role of Plastid Protein Phosphatase TAP38 in LHCII Dephosphorylation and Thylakoid Electron Flow

Mathias Pribil^{1,2}, Paolo Pesaresi³, Alexander Hertle¹, Roberto Barbato⁴, Dario Leister^{1*}

1 Plant Molecular Biology (Botany), Department Biology I, Ludwig-Maximilians-Universität, Munich, Germany, **2** Mass Spectrometry Unit, Department Biology I, Ludwig-Maximilians-Universität, Munich, Germany, **3** Department of Biomolecular Sciences and Biotechnology, University of Milan, Milan, Italy, **4** Department of Environmental and Life Sciences, Università del Piemonte Orientale, Alessandria, Italy

Abstract

Short-term changes in illumination elicit alterations in thylakoid protein phosphorylation and reorganization of the photosynthetic machinery. Phosphorylation of LHCII, the light-harvesting complex of photosystem II, facilitates its relocation to photosystem I and permits excitation energy redistribution between the photosystems (state transitions). The protein kinase STN7 is required for LHCII phosphorylation and state transitions in the flowering plant *Arabidopsis thaliana*. LHCII phosphorylation is reversible, but extensive efforts to identify the protein phosphatase(s) that dephosphorylate LHCII have been unsuccessful. Here, we show that the thylakoid-associated phosphatase TAP38 is required for LHCII dephosphorylation and for the transition from state 2 to state 1 in *A. thaliana*. In *tap38* mutants, thylakoid electron flow is enhanced, resulting in more rapid growth under constant low-light regimes. *TAP38* gene overexpression markedly decreases LHCII phosphorylation and inhibits state 1→2 transition, thus mimicking the *stn7* phenotype. Furthermore, the recombinant TAP38 protein is able, in an in vitro assay, to directly dephosphorylate LHCII. The dependence of LHCII dephosphorylation upon TAP38 dosage, together with the in vitro TAP38-mediated dephosphorylation of LHCII, suggests that TAP38 directly acts on LHCII. Although reversible phosphorylation of LHCII and state transitions are crucial for plant fitness under natural light conditions, LHCII hyperphosphorylation associated with an arrest of photosynthesis in state 2 due to inactivation of TAP38 improves photosynthetic performance and plant growth under state 2-favoring light conditions.

Citation: Pribil M, Pesaresi P, Hertle A, Barbato R, Leister D (2010) Role of Plastid Protein Phosphatase TAP38 in LHCII Dephosphorylation and Thylakoid Electron Flow. PLoS Biol 8(1): e1000288. doi:10.1371/journal.pbio.1000288

Academic Editor: Joanne Chory, The Salk Institute for Biological Studies, United States of America

Received: August 24, 2009; **Accepted:** December 11, 2009; **Published:** January 26, 2010

Copyright: © 2010 Pribil et al. This is an open-access article distributed under the terms of the Creative Commons Attribution License, which permits unrestricted use, distribution, and reproduction in any medium, provided the original author and source are credited.

Funding: This work was supported by the European Community (Human Potential Programme under contract HPRN-CT-2002-00248 [PSICO]) and the Deutsche Forschungsgemeinschaft (grants DL 1265/8 and /9; SFB-TR1 B8). The funders had no role in study design, data collection and analysis, decision to publish, or preparation of the manuscript.

Competing Interests: The authors have declared that no competing interests exist.

Abbreviations: F_{M1} , maximum fluorescence in state 1; F_{M2} , maximum fluorescence in state 2; F_v/F_m , the maximum quantum yield of photosystem II; Φ_{II} , effective quantum yield of photosystem II; PAR, photosynthetically active radiation; PSI, photosystem I; PSII, photosystem II; qT, the degree of quenching of chlorophyll fluorescence due to state transitions; WT, wild type

* E-mail: leister@lrz.uni-muenchen.de

Introduction

Owing to their sessile life style, plants have to cope with environmental changes in their habitats, such as fluctuations in the incident light. Changes in light quantity or quality (i.e., spectral composition) result in imbalanced excitation of the two photosystems and decrease the efficiency of the photosynthetic light reactions. Plants can counteract such excitation imbalances within minutes by a mechanism called *state transitions*, which depends on the reversible association of the mobile pool of major light-harvesting (LHCII) proteins with photosystem II (state 1) or photosystem I (PSI) (state 2) (reviewed in [1–5]). In detail, the accumulation of phosphorylated LHCII (pLHCII), stimulated in low white light, or by light of wavelengths specifically exciting PSII (red light), causes association of pLHCII with PSI (state 2), thus directing additional excitation energy to PSI. Conditions like darkness or light of wavelengths specifically exciting PSI (far-red light), as well as high intensities of white light, stimulate pLHCII dephosphorylation and its migration to PSII (state 1), thus redirecting excitation energy to PSII.

LHCII phosphorylation and state transitions have been extensively studied in the green alga *Chlamydomonas reinhardtii* and

the flowering plant *Arabidopsis thaliana* [2,4–6]. In *C. reinhardtii*, the impact of state transitions on interphotosystem energy balancing and on promoting cyclic electron flow is well established [2,5]. In flowering plants, however, the physiological significance of state transitions is less clear, because their mobile LHCII pools are significantly smaller than those in green algae [7,8]. Thus, *A. thaliana* mutant plants impaired in state transitions are only marginally affected in their development and fitness [9–11], even under fluctuating light or field conditions [12,13]. However, when *Arabidopsis* state transition mutants are perturbed in linear electron flow, effects on plant performance and growth rate become evident [14], indicating that also in flowering plants, state transitions are physiologically relevant.

The protein kinase responsible for phosphorylating LHCII is membrane bound and activated upon reduction of the cytochrome *b₆/f* (Cyt *b₆/f*) complex via the plastoquinone (PQ) pool under state 2-promoting light conditions (low white light or red light) [15,16]. PQ oxidizing conditions induced by state 1-promoting light conditions (dark or far-red light) inactivate the LHCII kinase and result in association of pLHCII with PSII (state 1, reviewed in [4,5]). The LHCII kinase activity, however, is also inactivated

Author Summary

Plants are able to adapt photosynthesis to changes in light levels by adjusting the activities of their two photosystems, the structures responsible for light energy capture. During a process called *state transitions*, a part of the photosynthetic complex responsible for light harvesting (the photosynthetic antennae) becomes reversibly phosphorylated and migrates between the photosystems to redistribute light-derived energy. The protein kinase responsible for phosphorylating photosynthetic antenna proteins was identified recently. However, despite extensive biochemical efforts to isolate the enzyme that catalyzes the corresponding dephosphorylation reaction, the identity of this protein phosphatase has remained unknown. In this study, we identified and characterized the thylakoid-associated phosphatase TAP38. We first demonstrate by spectroscopic measurements that the redistribution of excitation energy between photosystems that are characteristic of state transitions do not take place in plants without a functional TAP38 protein. We then show that the phosphorylation of photosynthetic antenna proteins is markedly increased in plants without TAP38, but decreased in plants that express more TAP38 protein than wild-type plants. This, together with the observation that addition of recombinant TAP38 decreases the level of antenna protein phosphorylation in an *in vitro* assay, suggests that TAP38 directly acts on the photosynthetic antenna proteins as the critical phosphatase regulating state transitions. Moreover, in plants without TAP38, photosynthetic electron flow is enhanced, resulting in more rapid growth under constant low-light regimes, thus providing the first instance of a mutant plant with improved photosynthesis.

under high white light conditions, when the stromal reduction state is very high. *In vitro* and, more recently, *in vivo* studies suggest that suppression of LHCII kinase activity might be mediated by reduced thioredoxin [17,18]. In *C. reinhardtii* and *A. thaliana*, the orthologous thylakoid protein kinases Stt7 and STN7, respectively, are required for LHCII phosphorylation and state transitions [12,19]. Coimmunoprecipitation assays showed that the Stt7 kinase interacts with Cyt *b₆/f*, PSI, and LHCII [17], suggesting that Stt7 (and STN7 in *Arabidopsis*) directly phosphorylates LHCII, rather than being part of a Stt7/STN7-dependent phosphorylation cascade.

Under PQ oxidizing conditions when the LHCII kinase becomes inactivated, pLHCII is dephosphorylated by the action of an as-yet unknown protein phosphatase, thus allowing the association of the mobile fraction of LHCII with PSII (state 1) [5,7]. For many years, attempts were undertaken to elucidate the characteristics and to identify the LHCII protein phosphatase(s). By means of biochemical approaches [20–22], it was shown that protein phosphatases of different families must be involved in the reversible phosphorylation of thylakoid phosphoproteins. A PP2A-like phosphatase was postulated to be responsible for the dephosphorylation of the PSII core proteins [23], whereas the LHCII phosphatase activity was shown to be dependent on the presence of divalent cations and not to be inhibited by microcystin and okadaic acid [21,22]. These findings strongly suggested an involvement of a PP2C-type phosphatase in pLHCII dephosphorylation [24].

Here, we show that the thylakoid protein phosphatase TAP38 is required for pLHCII dephosphorylation and state transitions. In plants with markedly reduced TAP38 levels, hyperphosphoryla-

tion of LHCII is associated with enhanced thylakoid electron flow, resulting in more rapid growth under constant low-light regimes. Together with the results of an *in vitro* dephosphorylation assay, our data indicate that TAP38 dephosphorylates pLHCII directly.

Results

Screening for Candidate LHCII Phosphatases

To identify the LHCII phosphatase, we systematically isolated loss-of-function mutants for known chloroplast protein phosphatases and assessed their capacity to dephosphorylate pLHCII (see below for details). However, none of the nine protein phosphatases At3g52180 (DSP4/SEX4), At4g21210 (AtRP1), At1g07160, At3g30020, At4g33500, At1g67820, At2g30170, At3g10940, or At4g03415, demonstrated to reside in the chloroplast [25–29], qualified as the LHCII phosphatase (unpublished data). Next, we extended our search to protein phosphatases tentatively identified as chloroplast proteins by proteomic analyses in *A. thaliana* [30,31]. Of those, the serine/threonine protein phosphatase At4g27800 turned out to be the most promising candidate.

At4g27800.1 (TAP38) Is a Thylakoid-Associated Protein Phosphatase

Proteins with high homology to At4g27800 exist in mosses and higher plants, but not in algae or prokaryotes. Furthermore, At4g27800 and its homologs share a predicted N-terminal chloroplast transit peptide (cTP), a putative transmembrane domain at their very C-terminus and a protein phosphatase 2C signature (Figure 1). For *A. thaliana*, three *At4g27800* mRNAs are predicted (Figure S1A). To verify their existence and to distinguish between the different splice forms, reverse-transcriptase PCR analyses were performed. Only *At4g27800.1*, and much less *At4g27800.2*, were detectable in leaves, whereas for the *At4g27800.3* splice variant, no signal could be obtained (Figure S1B).

In protoplasts transfected with *At4g27800.1* fused to the coding sequence for the red fluorescent protein (RFP) [32], the fusion protein localized to chloroplasts (Figure 2A). Chloroplast import assays with the radioactively labeled At4g27800.1 protein confirmed the uptake into the chloroplast with concomitant removal of its cTP. Mature At4g27800.1 has a molecular weight of ~38 kDa (Figure 2B). Immunoblot analysis using a specific antibody raised against the mature At4g27800.1 protein (Figure 2C) detected the protein in thylakoid preparations but not in stromal fractions. It is noteworthy, that the putative translation products At4g27800.2 and At4g27800.3 (~32 kDa) were undetectable (Figure 2C). At4g27800.1 is therefore the major isoform in leaves, and was renamed TAP38 (Thylakoid-Associated Phosphatase of 38 kDa).

TAP38 Expression in Wild-Type, *tap38* Mutant, and TAP38 Overexpressor Plants

Two *tap38* insertion mutants, *tap38-1* (SAIL_514_C03) [33] and *tap38-2* (SALK_025713) [34], were obtained from T-DNA insertion collections (Figure S1A). In *tap38-1* and *tap38-2* plants, amounts of *TAP38* transcripts were severely reduced, to 10% and 13% of WT levels, respectively (Figure 3A). Conversely, in transgenic lines carrying the *TAP38* coding sequence under control of the 35S promoter of Cauliflower Mosaic Virus (*oeTAP38*), levels of *TAP38* mRNA were much higher than in wild type (WT) (Figure 3A). TAP38 protein concentrations reflected the abundance of *TAP38* transcripts: *tap38-1* and *tap38-2* thylakoids had <5% and ~10% of WT levels, respectively, whereas the *oeTAP38* plants displayed >20-fold overexpression on

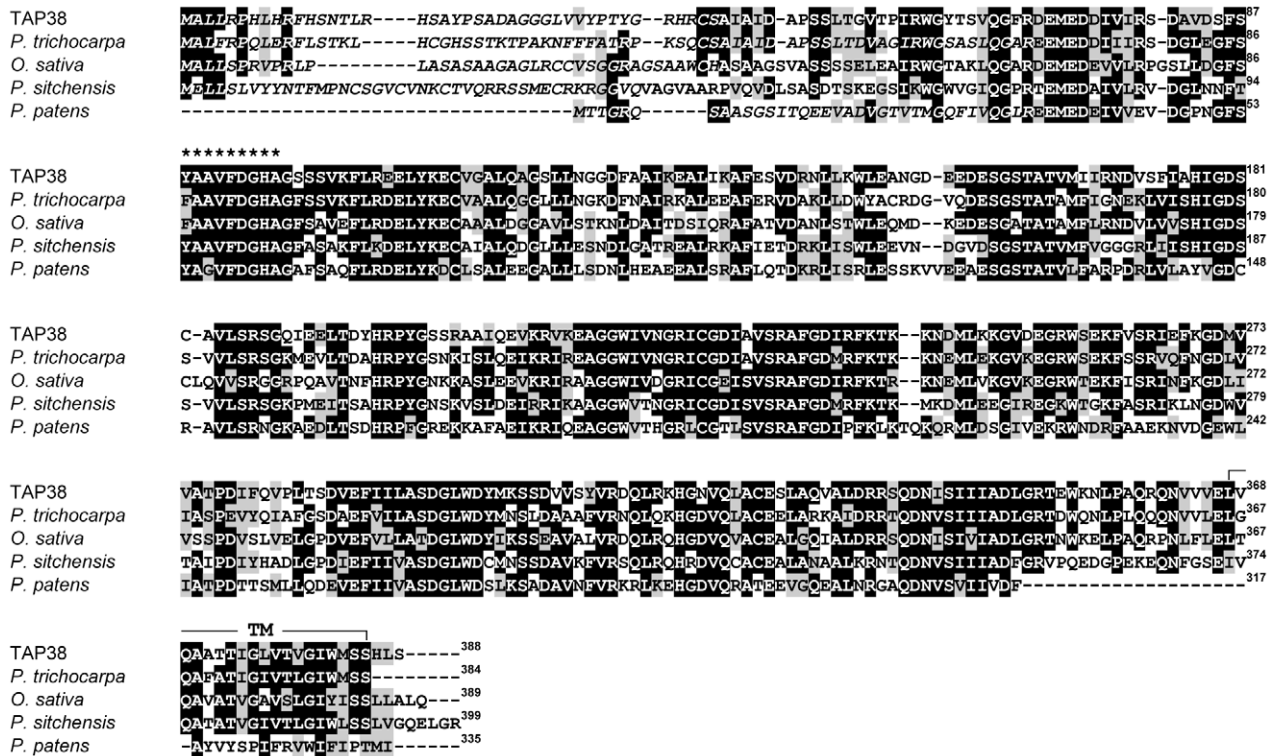


Figure 1. Comparison of the TAP38 sequence with those of related proteins from higher plants and moss. The amino acid sequence of the *Arabidopsis* TAP38 protein (At4g27800) was compared with related sequences from *Populus trichocarpa* (POPTRDRAFT_250893), *Oryza sativa* (Os01g0552300), *Picea sitchensis* (GenBank: EF676359.1), and *Physcomitrella patens* (PHYPADRAFT_113608). Black boxes highlight strictly conserved amino acids, and gray boxes closely related ones. Amino acids that constitute the protein phosphatase 2C signature are indicated by asterisks. Putative chloroplast transit peptides (cTPs) are indicated in italics, and the potential transmembrane domain (TM) is highlighted. doi:10.1371/journal.pbio.1000288.g001

the protein level (Figure 3B). TAP38 protein levels were also determined under light conditions relevant for state transitions (see Materials and Methods). In WT plants, TAP38 was constitutively expressed at similar levels under all light conditions applied (Figure 3C).

TAP38 Is Required for State Transitions

To determine whether TAP38 is involved in state transitions, chlorophyll fluorescence was measured in WT, *tap38*, and *oeTAP38* leaves (Figure 4A). Plants were exposed to light conditions that stimulate either state 2 (red light) or state 1 (far-red light) [35,36], and the corresponding maximum fluorescence in state 2 (F_{M2}) and in state 1 (F_{M1}) values were determined. Because the light intensity chosen to induce state transitions did not elicit photoinhibition (as monitored by measurements of the maximum quantum yield [F_v/F_M]), changes in F_M , the maximum fluorescence, could be attributed to state transitions alone. This allowed us to calculate the degree of quenching of chlorophyll fluorescence due to state transitions (qT) [36]. In the *tap38* mutants, qT was markedly decreased (*tap38-1*, 0.01 ± 0.003 ; *tap38-2*, 0.03 ± 0.001 ; WT, 0.10 ± 0.001). In *tap38-1* plants complemented with the TAP38 genomic sequence (including its native promoter), qT values were normal, confirming that state transitions require TAP38. Interestingly, *oeTAP38* plants exhibited qT values of about 0.01 ± 0.001 , indicating that both absence and excess of TAP38 interfere with the ability to undergo reversible state transitions.

To determine the antenna sizes of PSII and PSI, 77K fluorescence emission spectra were measured under state 1

(exposure to far-red light) and state 2 (low light) conditions as described [11,12,37] (Figure 4B). The spectra were normalized at 685 nm, the peak of PSII fluorescence. In WT, the transition from state 1 to state 2 was accompanied by a marked increase in relative PSI fluorescence at 730 nm, reflecting the redistribution of excitation energy from PSII to PSI. In contrast, in *tap38* leaves, the PSI fluorescence peak was relatively high even under state 1-promoting conditions, implying that the mutants were blocked in state 2—i.e., pLHCII should be predominantly attached to PSII. Additionally, under state 2-promoting light conditions, the PSI antenna size (expressed as F_{730}/F_{685}) was larger in *tap38* mutants than in WT (*tap38-1*, 1.47; *tap38-2*, 1.45; WT, 1.38; see also Table S1), arguing in favor of the idea that in *tap38* plants, a larger fraction of the mobile pool of LHCII can attach to PSII. On the contrary, in *oeTAP38* plants, the relative fluorescence of PSI hardly increased at all under conditions expected to induce the state 1→state 2 shift (Figure 4B; Table S1). This behavior resembles that of *stn7* mutants, which are blocked in state 1, i.e., with LHCII permanently attached to PSII [12].

Levels of LHCII Phosphorylation Correlate Inversely with TAP38 Concentrations

It is generally accepted that state transitions require reversible phosphorylation of LHCII [2,4,5]. Therefore, the phosphorylation state of LHCII was monitored under light conditions that favor state 1 (dark or far-red light treatment) or state 2 (low light). Plants with abnormal levels of TAP38, and WT plants were dark adapted for 16 h (state 1), then exposed to low light ($80 \mu\text{mol m}^{-2} \text{s}^{-1}$, 8 h) (state 2), and then to far-red light ($4.5 \mu\text{mol m}^{-2} \text{s}^{-1}$,

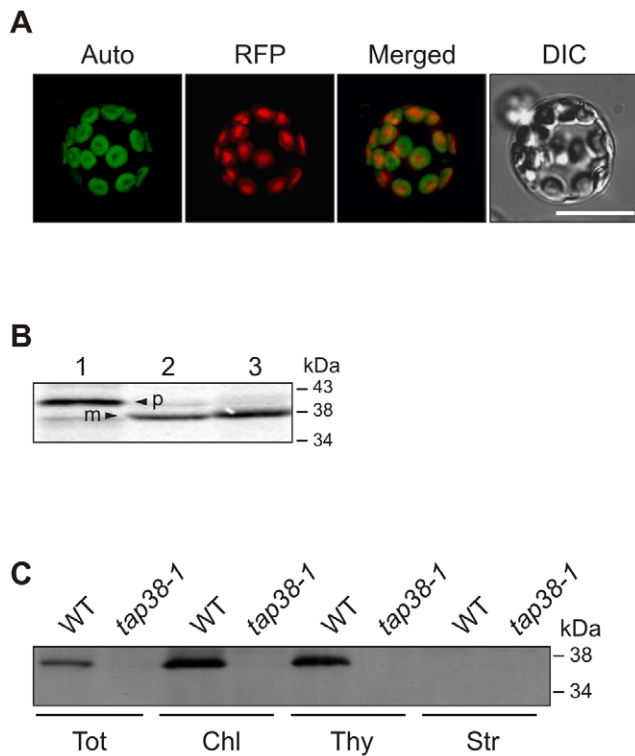


Figure 2. Subcellular localization of TAP38. (A) Full-length TAP38-RFP was transiently expressed in *Arabidopsis* protoplasts and visualized by fluorescence microscopy. Auto, chlorophyll autofluorescence; DIC, differential interference contrast image; merged, overlay of the two signals; RFP, fusion protein. Scale bar indicates 50 μ m. (B) 35 S-labeled TAP38 protein, translated in vitro (lane 1, 10% translation product), was incubated with isolated chloroplasts (lane 2), which were subsequently treated with thermolysin to remove adhering precursor proteins (lane 3), prior to SDS-PAGE and autoradiography. m, mature protein; p, precursor. (C) Immunoblot analyses of proteins from WT and *tap38-1* leaves. Equal protein amounts were loaded. Filters were immunolabeled with a TAP38-specific antibody. Chl, total chloroplasts; Str, stromal proteins; Thy, thylakoid proteins; Tot, total protein. doi:10.1371/journal.pbio.1000288.g002

740 nm) for up to 120 min to induce a return to state 1. Thylakoid proteins were isolated after each treatment, fractionated by sodium dodecyl sulfate (SDS)-PAGE, and analyzed with a phosphothreonine-specific antibody (Figure 5, left panels). WT plants showed the expected increase in pLHCII during the transition from state 1 (dark [D]) to state 2 (low light [LL]), followed by a progressive decrease in pLHCII upon exposure to far-red light (FR). In *tap38* mutants, levels of pLHCII were aberrantly high at all time points, whereas the *oeTAP38* plants again mimicked the *stn7* phenotype [9,12], displaying constitutively reduced levels of pLHCII.

Quantification of PSI-LHCI-LHCII Complex Formation under Varying TAP38 Concentrations

To directly visualize how alterations in LHCII phosphorylation in lines lacking or overexpressing TAP38 affect the distribution of the mobile LHCII fraction between the two photosystems, we subjected thylakoid protein complexes of plants adapted to state 1 (dark and far-red light treatments) or state 2 (low-light treatment) to nonreducing Blue-native (BN) PAGE [38] (Figure 5, right panels). In this assay, a pigment-protein complex of about 670 kDa, which represents pLHCII associated with the PSI-LHCI complex [14,38,39], can be visualized. Whereas in WT thylakoids,

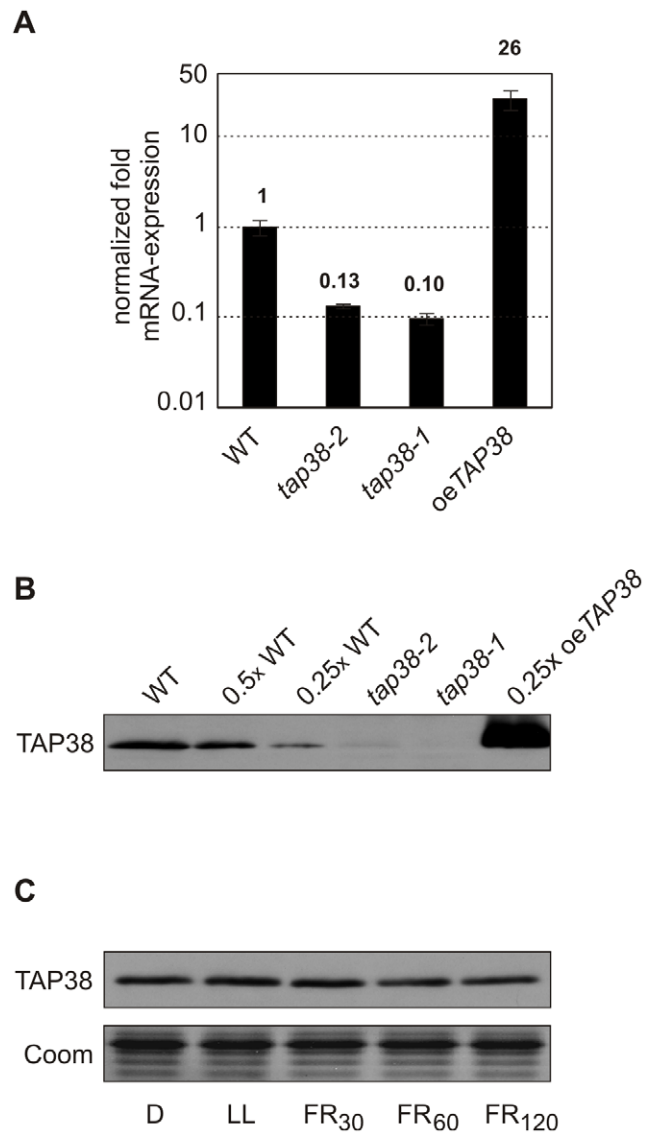


Figure 3. Expression of TAP38 in *tap38* mutant, TAP38 overexpressor, and WT plants. (A) Quantification of TAP38 mRNAs by real-time PCR in WT, *tap38-1*, *tap38-2*, and *oeTAP38* leaves using the primer combination 1 and 2 (as in Figure S1A and S1B). (B) Thylakoid proteins from WT and *tap38* mutants were loaded in the corresponding lanes. Reduced amounts of *oeTAP38* thylakoids, corresponding to 25% of WT amount were loaded in the lane marked as 0.25 \times *oeTAP38*. Additionally, decreasing levels of WT thylakoids were loaded in the lanes indicated as 0.5 \times WT and 0.25 \times WT. Filters were immunolabeled with a TAP38-specific antibody raised against the mature TAP38 protein. (C) Thylakoid membranes of WT plants exposed to different light conditions (see Figure 5) were separated by SDS-PAGE. Immunodecoration of the corresponding Western blot was performed using a TAP38-specific antibody raised against the mature protein. A detail of a replicate gel, corresponding to the LHCII migration region, stained with Coomassie Blue is shown as loading control. doi:10.1371/journal.pbio.1000288.g003

the 670-kDa complex was only observable under state 2 conditions (Figure 5A, right panel), as previously reported [14,39]; the constitutive phosphorylation of LHCII in the *tap38* mutants was associated with the presence of a prominent band for the 670-kDa complex under all light conditions (Figure 5B, right panel). The formation of the 670-kDa complex was totally prevented in *oeTAP38* plants with a block in state 1 and highly reduced levels of

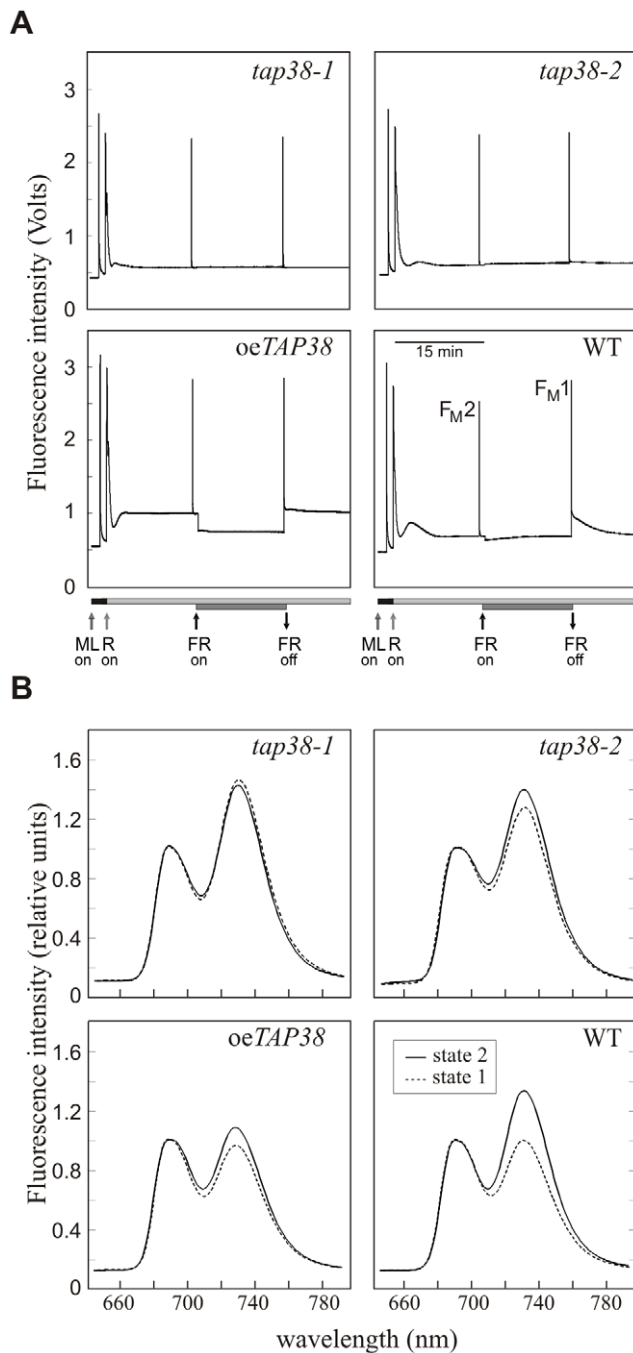


Figure 4. TAP38 is required for state transitions. (A) Red light (R) and red light supplemented with far-red (FR) light were used to induce transitions to state 2 and state 1, respectively. F_{M1} and F_{M2} represent maximal chlorophyll fluorescence levels in states 1 and 2, respectively. Horizontal bars indicate the length of illumination. Arrows point to the moment when the specific light is switched on/off. Traces are the average of 10 replicates. ML, measuring light. (B) Low-temperature (77 K) fluorescence emission spectra of thylakoids were recorded after exposure of plants to light inducing either state 1 (dashed lines, far-red light of 740 nm) or state 2 (solid lines, low light; $80 \mu\text{mol m}^{-2} \text{s}^{-1}$) (see also Materials and Methods). The excitation wavelength was 475 nm, and spectra were normalized with reference to peak height at 685 nm. Traces are the average of 10 replicates.
doi:10.1371/journal.pbio.1000288.g004

pLHCII (Figure 5C, right panel). Two-dimensional (2D) PA gel fractionation confirmed that the pigment-protein complex consists of PSI and LHCI subunits, together with a portion of pLHCII that associates with PSI upon state 1→state 2 transition in WT plants (Figure 6; [14]). Additionally, quantification of the different PSI complexes on 2D PA gels showed that the number of PSI complexes associated with LHCII was increased in the *tap38* mutants (Figures 6B and 6C), supporting the findings obtained from the 77K fluorescence analyses.

Recombinant TAP38 Is Able to Directly Dephosphorylate pLHCII

An *in vitro* dephosphorylation assay was established to assess the capability of TAP38 to directly dephosphorylate pLHCII. To this purpose, an N-terminal His-tag fusion of the TAP38 phosphatase was expressed in *Escherichia coli* and purified (see Materials and Methods). Solubilized thylakoids from *tap38-1* mutant plants were then fractionated by sucrose gradient ultracentrifugation, and the protein fraction enriched in pLHCII was isolated. Subsequently, the pLHCII pigment-protein complex was incubated at 30°C for 2 h either in the presence or absence of the recombinant TAP38 phosphatase. At the end of the incubation period, the reaction mixture was fractionated by SDS-PAGE and subjected to immunoblotting using a phosphothreonine-specific antibody (Figure 7). Clearly, the addition of the recombinant TAP38 decreased the level of LHCII phosphorylation by about 50% (relative to the untreated pLHCII sample). In the presence of the phosphatase inhibitor NaF, TAP38 addition did not markedly alter the phosphorylation level of LHCII. Taken together, these findings suggest that TAP38 is able to directly dephosphorylate pLHCII.

Plants without TAP38 Show Improved Photosynthesis and Growth under Low Light

When kept under low-light intensities ($80 \mu\text{mol m}^{-2} \text{s}^{-1}$) that favor state 2, *tap38* mutants grew larger than WT plants (Figure 8A), whereas *oeTAP38* plants behaved like WT (unpublished data). Detailed growth measurements revealed that the *tap38* mutants exhibited a constant growth advantage over WT plants, starting at the cotyledon stage (Figure 8B). Because this difference might be attributable to altered photosynthetic performance, parameters of thylakoid electron flow were measured. The fraction of Q_A (the primary electron acceptor of PSII) present in the reduced state ($1-qP$) was lower in *tap38-1* (0.06 ± 0.01) and *tap38-2* (0.07 ± 0.01) than in WT (0.10 ± 0.01), when both genotypes were grown as in Figure 8A and chlorophyll fluorescence was excited with $22 \mu\text{mol m}^{-2} \text{s}^{-1}$ actinic red light. Comparable differences in the redox state of the primary electron acceptor persisted up to $95 \mu\text{mol m}^{-2} \text{s}^{-1}$ actinic red light (Figure 8C), indicating that the *tap38* mutants can redistribute a larger fraction of energy to PSI, in accordance with the increase in its antenna size under state 2 light conditions (see Figure 4B; Table S1 and Figure 6). This idea was supported by measurements of the maximum (F_V/F_M) and effective (Φ_{II}) quantum yields of PSII. F_V/F_M remained unaltered in mutant plants (see Figure 8D, dark-adapted plants, photosynthetically active radiation [PAR]=0), indicating WT-like efficiency of mutant PSII complexes. However, Φ_{II} was increased in *tap38-1* (0.75 ± 0.01) and *tap38-2* (0.73 ± 0.02) relative to WT (0.72 ± 0.01), suggesting that electron flow through the thylakoids was more efficient in *tap38* mutants (Figure 8D). The improvement in photosynthetic performance of the *tap38* mutants was most pronounced under low and moderate illumination (Figures 8C and 8D), as expected from their growth phenotype.

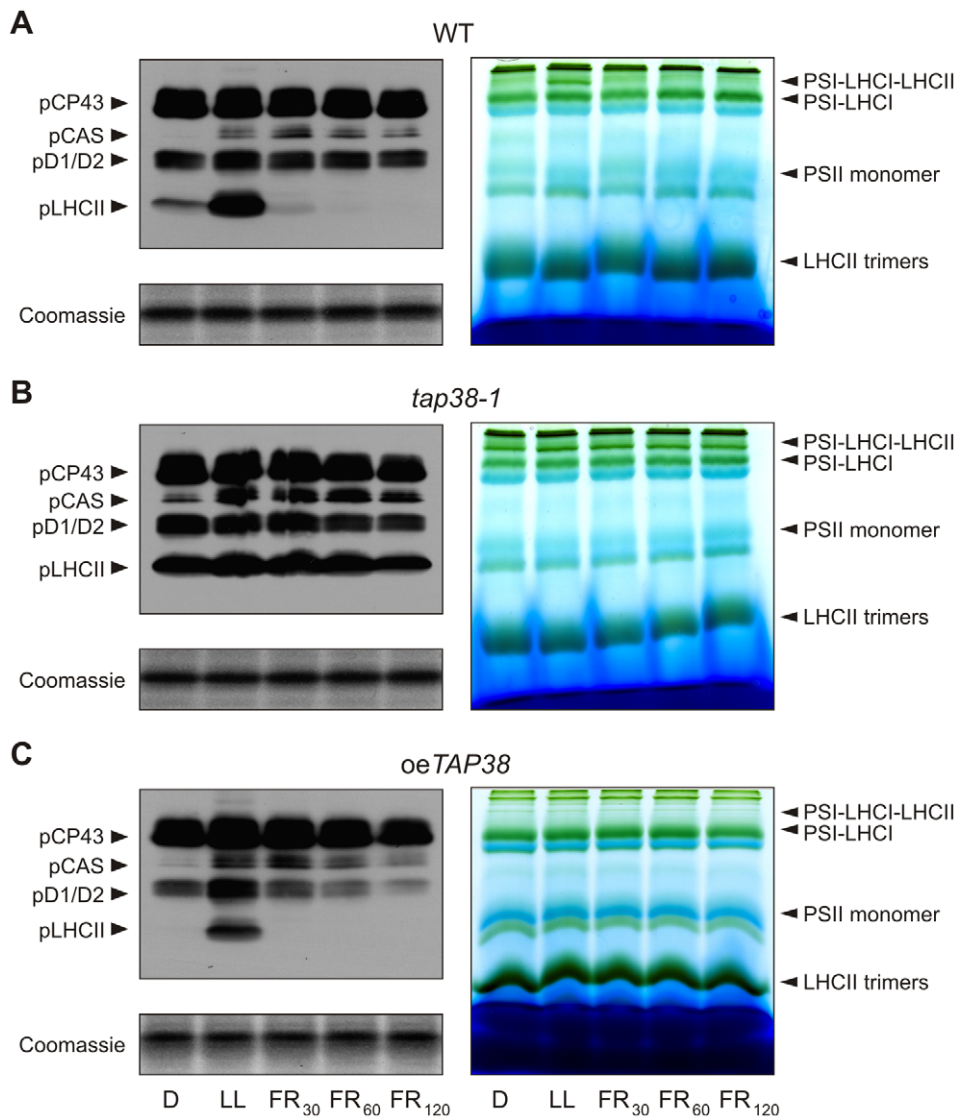


Figure 5. Levels of LHCII phosphorylation correlate inversely with TAP38 concentrations. Left panel, thylakoid proteins extracted from WT (A), *tap38-1* (B), and *oeTAP38* (C) plants kept in the dark (D; state 1), subsequently exposed to low light (LL; state 2), and then to far-red light for 30, 60, and 120 min (FR₃₀, FR₆₀, FR₁₂₀; state 1) were fractionated by SDS-PAGE. Phosphorylation of LHCII and PSII core proteins was detected by immunoblot analysis with a phosphothreonine-specific antibody. One out of three immunoblots for each genotype is shown. pCAS, phosphorylated CAS [44]; pCP43, phosphorylated CP43; pD1/D2, phosphorylated PSII-D1/D2; pLHCII, phosphorylated LHCI; Coomassie, portion of Coomassie-stained PA gels, identical to the ones blotted and corresponding to the LHCII migration region, were used as loading control. Right panel, thylakoid proteins of WT (A), *tap38-1* (B), and *oeTAP38* (C) plants treated as in the left panel were subjected to BN-PAGE analysis. Accumulation of the state 2-associated 670-kDa protein complex [14] correlates with the phosphorylation level of LHCII. Note that *tap38-2* behaved very similarly to *tap38-1* (data not shown). One out of three BN-PAGEs for each genotype is shown.
doi:10.1371/journal.pbio.1000288.g005

Discussion

Possible Modes of Action of TAP38

How does TAP38 control LHCII dephosphorylation? Three possibilities appear plausible: TAP38 (1) negatively regulates the activity of STN7 (e.g., by dephosphorylating it [40]), (2) dephosphorylates LHCII directly, or (3) forms part of a phosphorylation/dephosphorylation cascade that controls the activity of the LHCII kinase or phosphatase. The observation that *oeTAP38* plants, although showing a >20-fold increase in TAP38 levels, still exhibit residual LHCII phosphorylation (see Figure 5C), argues against the idea that TAP38 does inhibit STN7 by dephosphorylation. Differences in TAP38 levels resulted in a

clear change in pLHCII levels: although in *tap38* mutants a strong reduction in TAP38 led to a constantly high level of pLHCII and an increase in the amount of the PSI-LHCI-LHCII complex, strong overexpression of TAP38 (*oeTAP38*) caused the complete disappearance of pLHCII attached to PSI, although pLHCII was still present.

Taking these observations together, it appears that the TAP38 phosphatase acts specifically on pLHCII associated to PSI-LHCI complexes. Indeed, the dephosphorylation of pLHCII still attached to PSII under state 2-inducing light conditions seems unfavorable in terms of energy efficiency.

Interestingly, in WT where pLHCII levels can vary dramatically depending on the light conditions [9,12] (see also Figure 5A),

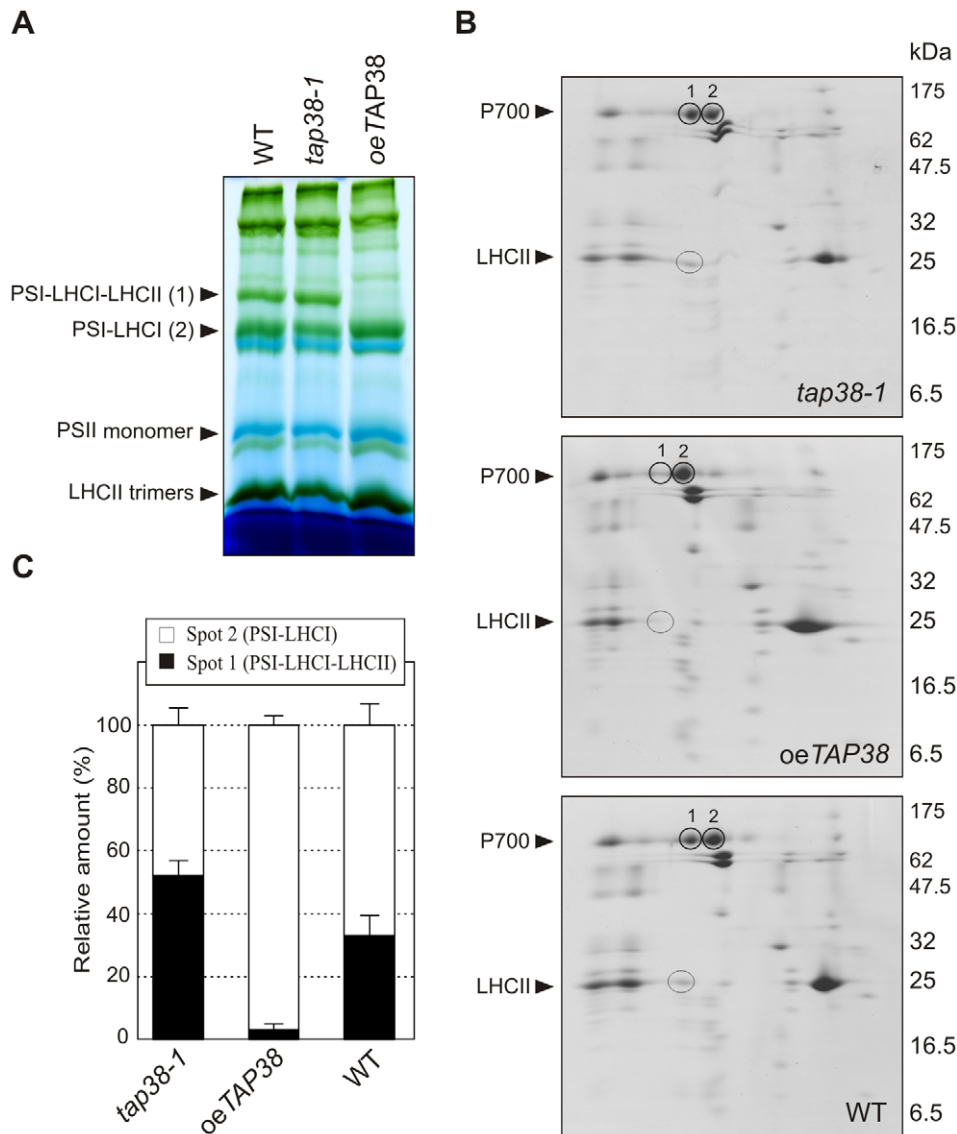


Figure 6. Quantification of PSI-LHCI and PSI-LHCI-LHCII complexes under state 2 conditions. (A) BN-PAGE of identical amounts of thylakoid proteins from WT, *tap38-1*, and *oeTAP38* plants adapted to state 2 (low light; $80 \mu\text{mol m}^{-2} \text{s}^{-1}$). Bands representing the PSI-LHCI-LHCII (1) and PSI-LHCI (2) complexes are indicated. The differences in the separation behavior of the BN-gel in comparison to the ones in Figure 5 are caused by the longer electrophoresis running time. (B) The WT, *tap38-1*, and *oeTAP38* lanes from the BN-PAGE in (A) were fractionated further by denaturing 2D-PAGE. Gels were stained with Coomassie Blue. LHCII, light-harvesting complex of PSII (the bands indicative for the PSI-LHCI-LHCII (1) and PSI-LHCI (2) complexes are encircled); P700, photosystem I reaction center. (C) Densitometric quantification of the spots representing PSI-LHCI-LHCII (spot 1) and PSI-LHCI (spot 2) in (B). Values are averages of three independent 2D gels for each genotype. Bars indicate standard deviations. Note that *tap38-2* behaves very similarly to *tap38-1* (data not shown). doi:10.1371/journal.pbio.1000288.g006

TAP38 seems to be constitutively expressed under the different light conditions applied (see Figure 3C). A plausible explanation for this is that TAP38 is constitutively active and directly responsible for the dephosphorylation of pLHCII. For that, TAP38 would need to be present in a certain concentration range (as it is the case for WT) to constantly dephosphorylate pLHCII. In agreement with that, thylakoid protein phosphatase reactions have been described as redox independent, leading to the conclusion that the redox dependency of LHCII phosphorylation is a property of the kinase reaction [41]. This, together with the observation that Stt7 levels increase under prolonged state 2 conditions (favoring LHCII phosphorylation) and decrease under state 1 conditions (favoring dephosphorylation of LHCII) [17],

argues in favor of the hypothesis that the LHCII kinase is the decisive factor in controlling the phosphorylation state of LHCII. Despite the obvious TAP38 dosage dependence of pLHCII dephosphorylation (see Figures 5 and 6), TAP38 activity could be regulated on other levels than only its abundance. However, the strong decrease or increase of TAP38 levels in *tap38* mutant and *oeTAP38* plants might interfere with other types of regulation in these genotypes.

Is TAP38 the Long-Sought LHCII Phosphatase?

As outlined above, the dependence of LHCII dephosphorylation upon TAP38 dosage—when comparing *tap38* mutants, WT, and TAP38 overexpressors—strongly suggests that TAP38

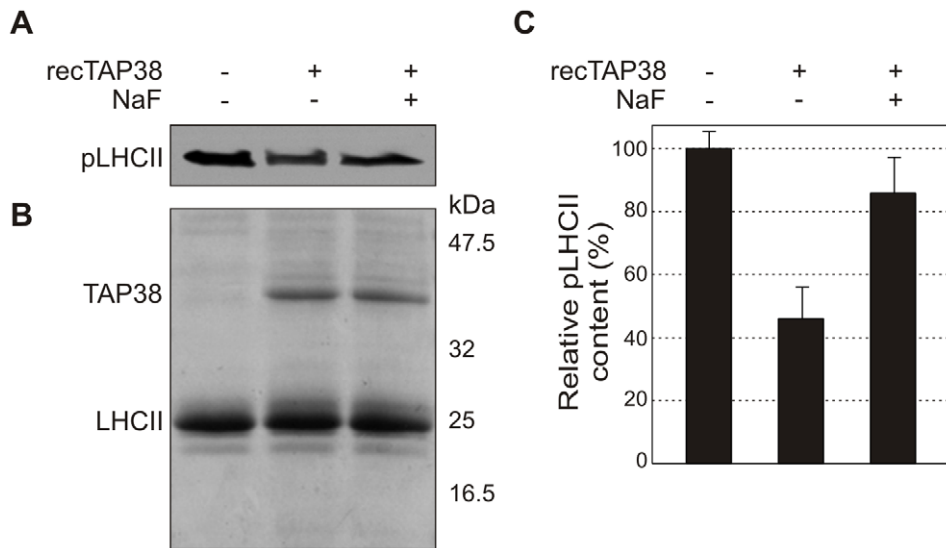


Figure 7. Recombinant TAP38 directly dephosphorylates pLHCII in vitro. (A) Equal amounts of pLHCII isolated from *tap38-1* mutant plants, treated with or without recombinant TAP38, were separated by SDS-PAGE and immunodecorated with phosphothreonine-specific antibodies. NaF (10 mM) was added to specifically inhibit phosphatase activity. (B) A replicate gel of the samples as in (A) was stained with Coomassie Blue as a loading control. The recombinant TAP38 protein and LHCII bands are shown. (C) Densitometric quantification of the bands in (A), representing the phosphorylation levels of LHCII under the different conditions. doi:10.1371/journal.pbio.1000288.g007

dephosphorylates pLHCII directly, particularly when it is associated with the PSI-LHCI complex. Alternatively, TAP38 could act in a phosphorylation/dephosphorylation cascade that controls the activity of the LHCII phosphatase. Although the latter hypothesis cannot be totally excluded, a set of evidences point to a direct role of TAP38 on LHCII phosphorylation. Indeed, our in vitro dephosphorylation assay clearly indicated that TAP38 can dephosphorylate pLHCII directly (see Figure 7). Moreover, as in the case of STN kinases, extensive efforts searching to identify other LHCII phosphatase candidates failed: knockout lines for all the protein phosphatases demonstrated to be located in the chloroplast [25–29] did not show any alteration in LHCII phosphorylation. Additionally, extensive biochemical studies did not reveal the existence of a complex network of phosphatases involved in LHCII dephosphorylation, but postulated the involvement of only two distinct chloroplast protein phosphatases from different families in the dephosphorylation of thylakoid phosphoproteins [20–23,42]. Our data support this notion, as shown by the absence of major alterations in the phosphorylation pattern of CP43, D1, and D2 subunits in *tap38* mutant plants (see Figure 5). Moreover, pLHCII dephosphorylation was suggested to be catalyzed by only two independent protein phosphatases, a membrane-bound one and a stromal protein phosphatase [42]. In contrast to this, our results clearly show that TAP38, a thylakoid-associated phosphatase, alone is responsible for LHCII dephosphorylation. Thus, although slightly leaky, the *tap38-1* mutants show a large fraction of LHCII in the phosphorylated state under all investigated conditions (see Figure 5). If a second LHCII phosphatase with redundant function would operate in chloroplasts, one would expect some residual dephosphorylation of pLHCII. A plausible explanation for the previously shown stromal pLHCII dephosphorylation activity [22] might be that during the preparation of stromal extracts, a significant portion of TAP38 was released from the thylakoid membrane into the stroma. Interestingly, TAP38 appears to influence also the phosphorylation levels of other thylakoid proteins, as shown by the higher phosphorylation of the CAS protein in *tap38-1* thylakoids (see Figure 5).

Taking these observations together, it appears that, as in the case of the STN kinases, two distinct phosphatases are needed to dephosphorylate LHCII and PSII core proteins. TAP38, similar to the STN7 kinase, seems to have a high specificity for pLHCII associated with PSI-LHCI complexes as substrate. The counterpart of STN8 [9,43], the PSII core-specific phosphatase, remains to be identified. However, as in the case of the STN7 and STN8 kinases, some degree of substrate overlap seems to exist also between the phosphatases, as shown by the more rapid dephosphorylation of PSII-D1/D2 subunits in the *TAP38* over-expressor lines exposed to far-red light conditions (see Figure 5C). Additionally, it is noteworthy that the activity of TAP38 does not seem to be restricted to STN7 substrates, as shown by its influence on CAS protein phosphorylation, previously reported to be a substrate of the STN8 kinase [44].

Uncoupling of LHCII Phosphorylation from PQ Redox State

It is known that an increase in the relative size of the reduced fraction of the plastoquinone pool (PQH₂) enhances phosphorylation of LHCII [1,5,39,45]. Depletion of TAP38 in *tap38* mutants, however, increases both LHCII phosphorylation (see Figure 5B) and PQ oxidation (see 1-qP values in Figure 8C). This discrepancy can be resolved by assuming that the enhanced oxidation of PQ caused by the increase in PSI antenna size (and LHCII phosphorylation) in *tap38* plants is not sufficient to down-regulate the LHCII kinase to such an extent that it can compensate for the decline in LHCII dephosphorylation.

How Can Absence of TAP38 Improve Photosynthesis and Growth?

The enhanced photosynthetic performance indicated by an increase in Φ_{II} and a decrease of 1-qP (see Figure 8C and 8D), as well as the growth advantage of the *tap38* mutants under constant moderate-light intensities that stimulate LHCII phosphorylation and state 2, can be attributed to the redistribution of a larger

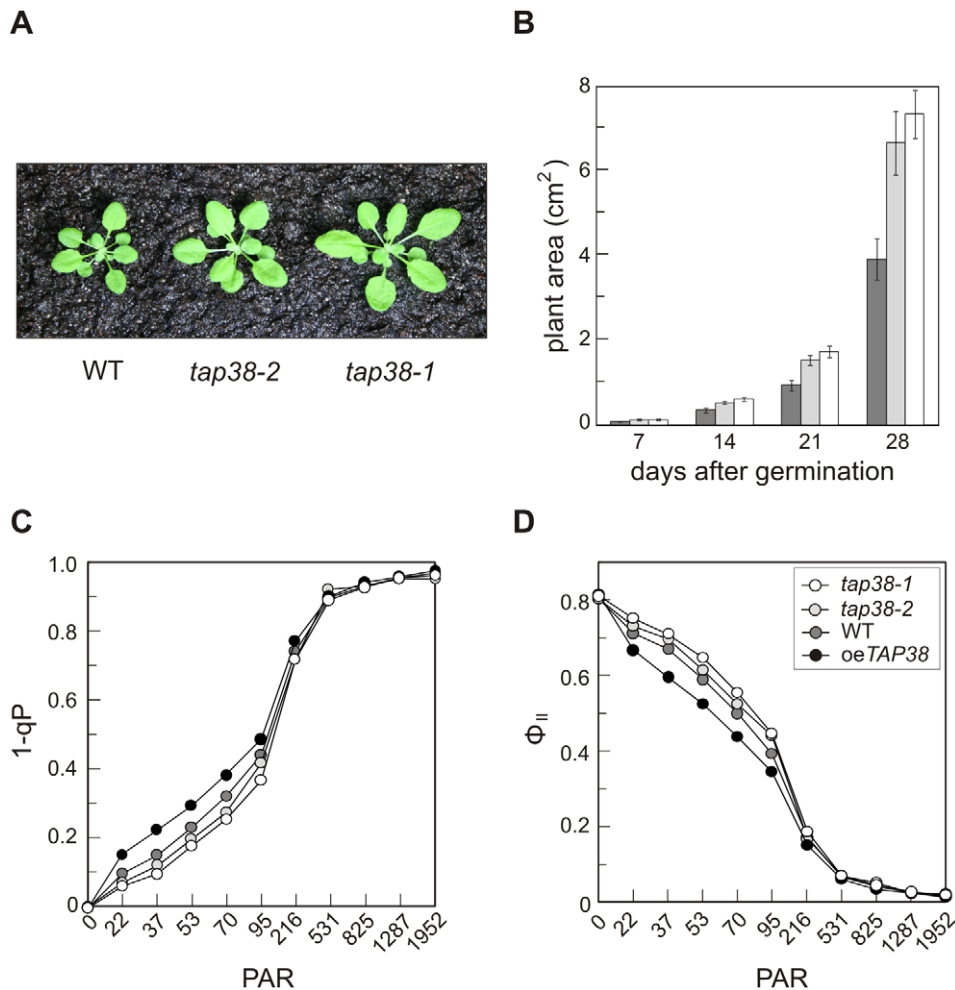


Figure 8. Growth characteristics and photosynthetic performance of *tap38* mutant plants. (A) Phenotypes of 4-wk-old *tap38-1*, *tap38-2*, and WT plants grown under low-light conditions ($80 \mu\text{mol m}^{-2}\text{s}^{-1}$) on a 12 h/12 h light/dark regime. (B) Growth curve. Leaf areas of 20 plants of each genotype (WT, grey bars; *tap38-1*, white bars; *tap38-2*, light grey bars) were measured over a period of 4 wk after germination. Mean values \pm standard deviations (SDs; bars) are shown. (C and D), Measurements of light dependence of the photosynthetic parameter 1-qP (C) and effective quantum yield of PSII (Φ_{II} ; [D]) of plants grown as in (A). WT, filled grey circles; *tap38-1*, open circles; *tap38-2*, filled light-grey circles; oeTAP38, filled black circles; PAR, photosynthetically active radiation in $\mu\text{mol m}^{-2} \text{s}^{-1}$. Average values were determined from five independent measurements (SD < 5%). doi:10.1371/journal.pbio.1000288.g008

fraction of energy to PSI. This is in accordance with the increase in PSI antenna size in *tap38* mutants when compared to WT plants (see Figure 4B, Table S1, and Figure 6). Therefore, it is straightforward to speculate that the enhanced PSI antenna size provides the *tap38* mutants with a more robust photosynthetic electron flow under conditions that preferentially excite PSII and induce state 2. As a consequence of the more balanced light reaction, the photosynthetic efficiency is improved resulting in an increased growth rate. However, the fitness advantage will revert under conditions that induce state 1, or under more natural conditions with fluctuating light; here, it can be expected that *tap38* mutants will perform less efficiently than the WT with respect to photosynthesis and growth, very similar to what has been observed for the *stn7* mutant [12,13].

Outlook

Taken together, future analyses should clarify which protein phosphatase is involved in the dephosphorylation of PSII core proteins and which are the counterparts of higher plant phosphatases, including TAP38, in *Chlamydomonas* (which appar-

ently lacks a *TAP38* ortholog). Additionally, further biochemical evidences that TAP38 (and STN7) uses pLHCII as a substrate will be very important for the complete molecular dissection of state transitions.

Materials and Methods

Plant Material and Growth Measurements

Procedures for plant propagation and growth measurements have been described elsewhere [46]. The *tap38-2* insertion line (SALK_025713) was identified in the SALK collection [34] (<http://signal.salk.edu/>), whereas insertion line *tap38-1* (SAIL_514_C03) originated from the Sail collection [33]. Both lines were identified by searching the insertion flanking database SIGNAL (<http://signal.salk.edu/cgi-bin/tdnaexpress>). To generate oeTAP38 lines, the coding sequence of *TAP38* was cloned into the plant expression vector pH2GW7 (Invitrogen). For complementation of the *tap38-1* mutant, the *TAP38* genomic DNA, together with 1 kb of its natural promoter, was ligated into the plant expression vector pP001-VS. The constructs were used to

transform flowers of Col-0 or *tap38-1* mutant plants by the floral dipping technique as described [47]. Transgenic plants, after selection for resistance to hygromycin (oe*TAP38*) or Basta herbicide (complemented *tap38-1*), were grown on soil in a climate chamber under controlled conditions (PAR: 80 $\mu\text{mol m}^{-2} \text{s}^{-1}$, 12/12 h dark/light cycles). The T2 generation of the oe*TAP38* plants was used for the experiments reported. Successful complementation of *tap38-1* mutants was confirmed by measurements of chlorophyll fluorescence and LHCII phosphorylation levels under light regimes promoting state transitions.

Subcellular Localization of the TAP38-dsRED Fusion in *Arabidopsis* Protoplasts

The full-length coding region of the *TAP38* gene was cloned into the vector pGJ1425, in frame with, and immediately upstream of the sequence encoding dsRED [32]. Isolation, transfection, and fluorescence microscopy of *A. thaliana* protoplasts were performed as described [48].

In Vitro Import of TAP38 into Pea Chloroplasts

The coding region of *TAP38* was cloned into the pGEM-Teasy vector (Promega) downstream of its SP6 promoter region, and mRNA was produced in vitro using SP6 RNA polymerase (MBI Fermentas). The TAP38 precursor protein was synthesized in a Reticulocyte Extract System (Flexi; Promega) in the presence of [³⁵S]methionine. Aliquots of the translation reaction were incubated with intact chloroplasts, and protein uptake was analyzed after treatment of isolated chloroplasts with thermolysin (Calbiochem) as described previously [49]. Labeled proteins were subjected to SDS-PAGE and detected by phosphorimaging (Typhoon; Amersham Biosciences).

cDNA Synthesis, Semiquantitative Reverse-Transcriptase PCR, and Real-Time PCR

Total RNA was extracted with the RNeasy Plant Mini Kit (QIAGEN) according to the manufacturer's instructions. cDNA was prepared from 1 μg of total RNA using the iScript cDNA Synthesis Kit (Bio-Rad) according to the manufacturer's instructions. For semiquantitative reverse-transcriptase PCR, cDNA was diluted 10-fold, and 3 μl of the dilution was used in a 20- μl reaction. Thermal cycling consisted of an initial step at 95°C for 3 min, followed by 30 cycles of 10 s at 95°C, 30 s at 55°C, and 10 s at 72°C. For real-time PCR analysis, 3 μl of the diluted cDNA was mixed with iQ SYBR Green Supermix (Bio-Rad). Thermal cycling consisted of an initial step at 95°C for 3 min, followed by 40 cycles of 10 s at 95°C, 30 s at 55°C, and 10 s at 72°C, after which a melting curve was performed. Real-time PCR was monitored using the iQ5 Multi-Color Real-Time PCR Detection System (Bio-Rad). All reactions were performed in triplicate with at least two biological replicates.

Protein Isolation and Immunoblot Analysis

Total protein extracts and proteins from total chloroplasts, thylakoids, and the stroma fraction were prepared from 4-wk-old leaves in the presence of 10 mM NaF as described [48,50]. Immunoblot analyses with phosphothreonine-specific antibodies (Cell Signaling) or polyclonal antibodies raised against the mature TAP38 protein were performed as described [45].

Blue-Native (BN)-PAGE and 2D Polyacrylamide Gel Electrophoresis (2D-PAGE)

For BN-PAGE, thylakoid membranes were prepared as described above. Aliquots corresponding to 100 μg of chlorophyll

were solubilized in solubilization buffer (750 mM 6-aminocaproic acid; 5 mM EDTA [pH 7]; 50 mM NaCl; 1.5% digitonin) for 1 h at 4°C. After centrifugation for 1 h at 21,000g, the solubilized material was fractionated by nondenaturing BN-PAGE at 4°C as described [38].

For 2D-PAGE, samples were fractionated in the first dimension by BN-PAGE as described above and subsequently by denaturing SDS-PAGE as described previously [51]. Densitometric analysis of the stained gels was performed using the Lumi Analyst 3.0 (Boehringer).

Measurements of State Transitions and 77 K Fluorescence

State transitions were measured by pulse amplitude modulation fluorometry (PAM) [35,36] and 77 K fluorescence emission analysis [12,37]. Plants adapted to state 1 conditions were obtained by incubation either in darkness or far-red light, whereas state 2 was induced by either red- or low-light illumination. Both state 1 and state 2 light-inducing conditions were used in different combinations, since they resulted in identical effects on state transitions. Additionally, there was no major reason to prefer one light setting to the other, except for the fact that the PAM fluorometer is equipped with red and far-red lights. For state transition measurements, five plants of each genotype were analyzed, and mean values and standard deviations were calculated. In vivo chlorophyll *a* fluorescence of single leaves was measured using the Dual-PAM 100 (Walz). Pulses (0.5 s) of red light (5,000 $\mu\text{mol m}^{-2} \text{s}^{-1}$) were used to determine the maximum fluorescence and the ratio $(F_M - F_0)/F_M = F_V/F_M$. Quenching of chlorophyll fluorescence due to state transitions (qT) was determined by illuminating dark-adapted leaves with red light (35 $\mu\text{mol m}^{-2} \text{s}^{-1}$, 15 min) and then measuring the maximum fluorescence in state 2 (F_{M2}). Next, state 1 was induced by adding far-red light (maximal light intensity corresponding to level 20 in the Dual-PAM setting, 15 min), and recording F_{M1} . qT was calculated as $(F_{M1} - F_{M2})/F_{M1}$ [36].

For 77 K fluorescence emission spectroscopy, the fluorescence spectra of thylakoids were recorded after irradiating plants with light that favored excitation of PSII (80 $\mu\text{mol m}^{-2} \text{s}^{-1}$, 8 h) or PSI (LED light of 740 nm wavelength, 4.6 $\mu\text{mol m}^{-2} \text{s}^{-1}$, 2 h). Thylakoids were isolated in the presence of 10 mM NaF as described [11], and 77 K fluorescence spectra were obtained by excitation at 475 nm using a Spex Fluorolog mod.1 fluorometer (Spex Industries). The emission between 600 and 800 nm was recorded, and spectra were normalized relative to peak height at 685 nm. Data frequency was of 0.5 nm with an integration time of 0.1 s.

In Vitro Dephosphorylation Assay

pLHCII was obtained from fractionation of *tap38-1* thylakoids by sucrose gradient ultracentrifugation as previously described [45]. The cDNA sequence of mature TAP38 was cloned into pET151 (Invitrogen), and recombinant TAP38 (recTAP38) was expressed in the *E. coli* strain BL21 with a N-terminal-6x His-tag. recTAP38 was purified under denaturing conditions following a Ni-NTA batch purification procedure according to the manufacturer's instructions (QIAGEN). After protein precipitation in 10% trichloroacetic acid (TCA) followed by three washing steps with absolute ethanol, around 500 μg of TAP38 protein were resuspended in 500 μl of 1% (w/v) lithium dodecyl sulfate (LDS), 12.5% (w/v) sucrose, 5 mM ϵ -aminocaproic acid, 1 mM benzamidine, and 50 mM HEPES KOH (pH 7.8), as previously described [52]. Subsequently, TAP38 protein was boiled for 2 min at 100°C and then transferred for 15 min at 25°C. Then,

dithiothreitol (DTT; 75 mM final concentration) was added, and the solution was subjected to three freezing-thawing cycles (20 min at -20°C , 20 min at -80°C , 20 min at -20°C , thawing in a ice-water bath, and 5 min at 25°C). After completion of the three freezing-thawing cycles, octyl-glucopyranoside (OGP; 1% [w/v] final concentration) was added, and the solution was kept on ice for 15 min. Afterwards, KCl (75 mM, final concentration) was added to precipitate the LDS detergent. After centrifugation at $16,000g$ at 4°C for 10 min, the supernatant containing the refolded TAP38 in the presence of 1% (w/v) OGP was collected. Subsequently, 1 μl of phosphatase was incubated together with pLHCII corresponding to 2 μg of total chlorophyll. The dephosphorylation reaction was performed in 50 μl containing 0.06% (w/v) dodecyl- β -D-maltoside, 5 mM Mg-acetate, 5 mM DTT, 100 mM HEPES (pH 7.8), at 37°C for 2 h as previously described [22]. The reaction mixture was loaded on a SDS-PAGE and immunodecorated with a phosphothreonine-specific antibody, as described above.

Supporting Information

Figure S1 Insertion alleles of *At4g27800* and their effects on splice variant expression. (A) T-DNA insertions in the *At4g27800* locus. The different coding sequences of the three splice variants are depicted as grey boxes. The respective 5' and 3' UTRs are shown in white. Introns are indicated as thin lines. Splice variants *At4g27800.1* (*TAP38*) and *At4g27800.3* can be distinguished due to an insertion of four additional nucleotides in exon 9 of *At4g27800.3* leading to a stop codon. Arrows (not drawn to scale) indicate the positions of primer pairs used in PCR analysis. Sequences of primers indicated as 1, 2, 3, and 4 are: *At4g27800.1/TAP38-At4g27800.2*-specific primer (No. 1): 5'-ACATGGGAATGTGCAGCTTG; *At4g27800.1/TAP38-At4g27800.2-At4g27800.3* (No. 2): 5'-GTGAAGACATC-

CATATGCCA; *At4g27800.2*-specific primer (No. 3): 5'-AA-TACCTCCTCAGCCTTTC; *At4g27800.3*-specific primer (No. 4): 5'-ACATGGGAATGTGCAGGCAA. (B) Semiquantitative reverse transcriptase (RT)-PCR analysis to verify the presence of the three splice variants in *Arabidopsis* WT leaves. Primer combinations employed in RT-PCR reactions are numbered as in (A). *Ubiquitin (UBI)* was amplified as a control for equal loading (Ubiquitin forward primer: 5'-GGAAAAAGGTCTGACC-GACA; Ubiquitin reverse: 5'-CTGTTCACGGAACCCAATTC). Aliquots (10 μl) of representative semiquantitative RT-PCR reactions (30 cycles) were electrophoresed on a 2% (w/v) agarose gel to differentiate between *At4g27800.1* (*TAP38*) and *At4g27800.2*. Note that for the *At4g27800.3* splice variant, no signal could be obtained.

Found at: doi:10.1371/journal.pbio.1000288.s001 (0.35 MB TIF)

Table S1 Energy distribution between PSI and PSII measured as the fluorescence emission ratio at 730 nm and 685 nm (F_{730}/F_{685}).

Found at: doi:10.1371/journal.pbio.1000288.s002 (0.04 MB DOC)

Acknowledgments

We thank Paul Hardy for critical comments on the manuscript; and the Salk Institute for making T-DNA insertion lines publicly available.

Author Contributions

The author(s) have made the following declarations about their contributions: Conceived and designed the experiments: MP PP DL. Performed the experiments: MP PP AH. Analyzed the data: MP PP AH DL. Contributed reagents/materials/analysis tools: RB. Wrote the paper: MP PP DL.

References

- Allen JF, Forsberg J (2001) Molecular recognition in thylakoid structure and function. *Trends Plant Sci* 6: 317–326.
- Eberhard S, Finazzi G, Wollman FA (2008) The dynamics of photosynthesis. *Annu Rev Genet* 42: 463–515.
- Haldrup A, Jensen PE, Lunde C, Scheller HV (2001) Balance of power: a view of the mechanism of photosynthetic state transitions. *Trends Plant Sci* 6: 301–305.
- Rochaix JD (2007) Role of thylakoid protein kinases in photosynthetic acclimation. *FEBS Lett* 581: 2768–2775.
- Wollman FA (2001) State transitions reveal the dynamics and flexibility of the photosynthetic apparatus. *EMBO J* 20: 3623–3630.
- Allen JF, Race HL (2002) Will the real LHC II kinase please step forward? *Sci STKE* 2002: PE43.
- Allen JF (1992) Protein phosphorylation in regulation of photosynthesis. *Biochim Biophys Acta* 1098: 275–335.
- Delosme R, Beal D, Joliot P (1994) Photoacoustic detection of flash-induced charge separation in photosynthetic systems: spectral dependence of the quantum yield. *Biochim Biophys Acta* 1185: 56–64.
- Bonardi V, Pesaresi P, Becker T, Schleiff E, Wagner R, et al. (2005) Photosystem II core phosphorylation and photosynthetic acclimation require two different protein kinases. *Nature* 437: 1179–1182.
- Lunde C, Jensen PE, Haldrup A, Knoetzel J, Scheller HV (2000) The PSI-H subunit of photosystem I is essential for state transitions in plant photosynthesis. *Nature* 408: 613–615.
- Tikkanen M, Piippo M, Suorsa M, Sirpio S, Mulo P, et al. (2006) State transitions revisited—a buffering system for dynamic low light acclimation of *Arabidopsis*. *Plant Mol Biol* 62: 779–793.
- Bellaïf S, Bameche F, Peltier G, Rochaix JD (2005) State transitions and light adaptation require chloroplast thylakoid protein kinase STN7. *Nature* 433: 892–895.
- Frenkel M, Bellaïf S, Rochaix JD, Jansson S (2007) Hierarchy amongst photosynthetic acclimation responses for plant fitness. *Physiol Plant* 129: 455–459.
- Pesaresi P, Hertle A, Pribil M, Kleine T, Wagner R, et al. (2009) *Arabidopsis* STN7 kinase provides a link between short- and long-term photosynthetic acclimation. *Plant Cell* 21: 2402–2423.
- Vener AV, VanKan PJM, Rich PR, Ohad I, Andersson B (1997) Plastoquinol at the quinol oxidation site of reduced cytochrome *bf* mediates signal transduction between light and protein phosphorylation: thylakoid protein kinase deactivation by a single-turnover flash. *Proc Natl Acad Sci U S A* 94: 1585–1590.
- Zito F, Finazzi G, Delosme R, Nitschke W, Picot D, et al. (1999) The Qo site of cytochrome *b₆f* complexes controls the activation of the LHCII kinase. *EMBO J* 18: 2961–2969.
- Lemelle S, Willig A, Depege-Fargeix N, Delessert C, Bassi R, et al. (2009) Analysis of the chloroplast protein kinase Stt7 during state transitions. *PLoS Biol* 7: e1000045. doi:10.1371/journal.pbio.1000045.
- Rintamäki E, Martinsuo P, Pursiheimo S, Aro EM (2000) Cooperative regulation of light-harvesting complex II phosphorylation via the plastoquinol and ferredoxin-thioredoxin system in chloroplasts. *Proc Natl Acad Sci U S A* 97: 11644–11649.
- Depege N, Bellaïf S, Rochaix JD (2003) Role of chloroplast protein kinase Stt7 in LHCII phosphorylation and state transition in *Chlamydomonas*. *Science* 299: 1572–1575.
- Hast T, Föllmann H (1996) Identification of two thylakoid-associated phosphatases with protein phosphatase activity in chloroplasts of the soybean (*Glycine max*). *J Photochem Photobiol B* 36: 313–319.
- Sun G, Bailey D, Jones MW, Markwell J (1989) Chloroplast thylakoid protein phosphatase is a membrane surface-associated activity. *Plant Physiol* 89: 238–243.
- Hammer MF, Sarath G, Markwell J (1995) Dephosphorylation of the thylakoid membrane light-harvesting complex II by a stromal protein phosphatase. *Photosynth Res* 45: 195–201.
- Vener AV, Rokka A, Fulgosi H, Andersson B, Herrmann RG (1999) A cyclophilin-regulated PP2A-like protein phosphatase in thylakoid membranes of plant chloroplasts. *Biochemistry* 38: 14955–14965.
- Cohen P (1989) The structure and regulation of protein phosphatases. *Annu Rev Biochem* 58: 453–508.
- Chastain CJ, Xu W, Parsley K, Sarath G, Hibberd JM, et al. (2008) The pyruvate, orthophosphate dikinase regulatory proteins of *Arabidopsis* possess a novel, unprecedented Ser/Thr protein kinase primary structure. *Plant J* 53: 854–863.
- Kerk D, Conley TR, Rodriguez FA, Tran HT, Nimick M, et al. (2006) A chloroplast-localized dual-specificity protein phosphatase in *Arabidopsis* contains a phylogenetically dispersed and ancient carbohydrate-binding domain, which binds the polysaccharide starch. *Plant J* 46: 400–413.

27. Niittyla T, Comparot-Moss S, Luc WL, Messerli G, Trevisan M, et al. (2006) Similar protein phosphatases control starch metabolism in plants and glycogen metabolism in mammals. *J Biol Chem* 281: 11815–11818.
28. Schliebner I, Pribil M, Zuhlke J, Dietzmann A, Leister D (2008) A survey of chloroplast protein kinases and phosphatases in *Arabidopsis thaliana*. *Curr Genomics* 9: 184–190.
29. Sokolov LN, Dominguez-Solis JR, Allary AL, Buchanan BB, Luan S (2006) A redox-regulated chloroplast protein phosphatase binds to starch diurnally and functions in its accumulation. *Proc Natl Acad Sci U S A* 103: 9732–9737.
30. Sun Q, Zybailov B, Majeran W, Friso G, Olinares PD, et al. (2009) PPDB, the Plant Proteomics Database at Cornell. *Nucleic Acids Res* 37: D969–974.
31. Zybailov B, Rutschow H, Friso G, Rudella A, Emanuelsson O, et al. (2008) Sorting signals, N-terminal modifications and abundance of the chloroplast proteome. *PLoS ONE* 3: e1994. doi:10.1371/journal.pone.0001994.
32. Jach G, Binot E, Frings S, Luxa K, Schell J (2001) Use of red fluorescent protein from *Dicosoma* sp. (dsRED) as a reporter for plant gene expression. *Plant J* 28: 483–491.
33. Sessions A, Burke E, Presting G, Aux G, McElver J, et al. (2002) A high-throughput *Arabidopsis* reverse genetics system. *Plant Cell* 14: 2985–2994.
34. Alonso JM, Stepanova AN, Leisse TJ, Kim CJ, Chen H, et al. (2003) Genome-wide insertional mutagenesis of *Arabidopsis thaliana*. *Science* 301: 653–657.
35. Jensen PE, Gilpin M, Knoetzel J, Scheller HV (2000) The PSI-K subunit of photosystem I is involved in the interaction between light-harvesting complex I and the photosystem I reaction center core. *J Biol Chem* 275: 24701–24708.
36. Ruban AV, Johnson MP (2009) Dynamics of higher plant photosystem cross-section associated with state transitions. *Photosynth Res* 99: 173–183.
37. Tikkanen M, Nurmi M, Suorsa M, Danielsson R, Mamedov F, et al. (2008) Phosphorylation-dependent regulation of excitation energy distribution between the two photosystems in higher plants. *Biochim Biophys Acta* 1777: 425–432.
38. Heinemeyer J, Eubel H, Wehmhoner D, Jansch L, Braun HP (2004) Proteomic approach to characterize the supramolecular organization of photosystems in higher plants. *Phytochemistry* 65: 1683–1692.
39. Pesaresi P, Lunde C, Jahns P, Tarantino D, Meurer J, et al. (2002) A stable LHCI-PSI aggregate and suppression of photosynthetic state transitions in the *psae1-1* mutant of *Arabidopsis thaliana*. *Planta* 215: 940–948.
40. Heazlewood JL, Durek P, Hummel J, Selbig J, Weckwerth W, et al. (2008) PhosPhAt: a database of phosphorylation sites in *Arabidopsis thaliana* and a plant-specific phosphorylation site predictor. *Nucleic Acids Res* 36: D1015–1021.
41. Silverstein T, Cheng L, Allen JF (1993) Chloroplast thylakoid protein phosphatase reactions are redox-independent and kinetically heterogeneous. *FEBS Lett* 334: 101–105.
42. Hammer MF, Sarath G, Osterman JC, Markwell J (1995) Assessing modulations of stromal and thylakoid light-harvesting complex-II phosphatase activities with phosphopeptide substrates. *Photosynth Res* 44: 107–115.
43. Vainonen JP, Hansson M, Vener AV (2005) STN8 protein kinase in *Arabidopsis thaliana* is specific in phosphorylation of photosystem II core proteins. *J Biol Chem* 280: 33679–33686.
44. Vainonen JP, Sakuragi Y, Stael S, Tikkanen M, Allahverdiyeva Y, et al. (2008) Light regulation of CaS, a novel phosphoprotein in the thylakoid membrane of *Arabidopsis thaliana*. *FEBS J* 275: 1767–1777.
45. Ihnatowicz A, Pesaresi P, Lohrig K, Wolters D, Muller B, et al. (2008) Impaired photosystem I oxidation induces STN7-dependent phosphorylation of the light-harvesting complex I protein Lhca4 in *Arabidopsis thaliana*. *Planta* 227: 717–722.
46. Leister D, Varotto C, Pesaresi P, Niwergall A, Salamini F (1999) Large-scale evaluation of plant growth in *Arabidopsis thaliana* by non-invasive image analysis. *Plant Physiol Biochem* 37: 671–678.
47. Clough SJ, Bent AF (1998) Floral dip: a simplified method for *Agrobacterium*-mediated transformation of *Arabidopsis thaliana*. *Plant J* 16: 735–743.
48. DalCorso G, Pesaresi P, Masiero S, Asceva E, Schunemann D, et al. (2008) A complex containing PGRL1 and PGR5 is involved in the switch between linear and cyclic electron flow in *Arabidopsis*. *Cell* 132: 273–285.
49. Bolter B, Soll J (2007) Import of plastid precursor proteins into pea chloroplasts. *Methods Mol Biol* 390: 195–206.
50. Bassi R, dal Belin Peruffo A, Barbato R, Ghisi R (1985) Differences in chlorophyll-protein complexes and composition of polypeptides between thylakoids from bundle sheaths and mesophyll cells in maize. *Eur J Biochem* 146: 589–595.
51. Pesaresi P, Varotto C, Meurer J, Jahns P, Salamini F, et al. (2001) Knock-out of the plastid ribosomal protein L11 in *Arabidopsis*: effects on mRNA translation and photosynthesis. *Plant J* 27: 179–189.
52. Giuffra E, Cugini D, Croce R, Bassi R (1996) Reconstitution and pigment-binding properties of recombinant CP29. *Eur J Biochem* 238: 112–120.